The Thai Journal of Veterinary Medicine

Volume 56
Issue 1 *January - March*

Article 17

February 2026

MicroRNA expression in putative cancer stem cells isolated from canine mammary gland tumour cells with differing sensitivity to doxorubicin

Kabiru Sahabi
Faculty of Veterinary Medicine, Universiti Putra Malaysia; Faculty of Veterinary Medicine, Universiti Malaysia Kelantan, kabirukalgo@gmail.com

Gayathri Thevi Selvarajah
Faculty of Veterinary Medicine; Institute of Biosciences, Universiti Putra Malaysia, gayathri@upm.edu.my

Mohd Mokrish Md Ajat
Faculty of Veterinary Medicine, Universiti Putra Malaysia, mokrish@upm.edu.my

Rasedee Abdullah
Faculty of Veterinary Medicine, Universiti Putra Malaysia, rasedee@upm.edu.my

Cheah Y. Kqueen
Faculty of Medicine and Health Sciences, Universiti Putra Malaysia, ykcheah@upm.edu.my

Recommended Citation

Sahabi, Kabiru; Selvarajah, Gayathri Thevi; Ajat, Mohd Mokrish Md; Abdullah, Rasedee; and Kqueen, Cheah Y. (2026) "MicroRNA expression in putative cancer stem cells isolated from canine mammary gland tumour cells with differing sensitivity to doxorubicin," *The Thai Journal of Veterinary Medicine*: Vol. 56: Iss. 1, Article 17.
DOI: https://doi.org/10.56808/2985-1130.3923
Available at: https://digital.car.chula.ac.th/tjvm/vol56/iss1/17

Original Article

MicroRNA expression in putative cancer stem cells isolated from canine mammary gland tumour cells with differing sensitivity to doxorubicin

Kabiru Sahabi[1,2] Gayathri Thevi Selvarajah[1,3*] Mohd Mokrish Md Ajat[4]

Rasedee Abdullah[5] Cheah Y. Kqueen[6]

Abstract

Cancer stem cells (CSCs) are capable of initiating tumour development and causing recurrence after treatment. The objective of this study was to determine the miRNAs, downstream target mRNAs, and signalling pathways in CSCs isolated from doxorubicin-sensitive and doxorubicin-resistant canine mammary adenocarcinoma cell lines. MicroRNA expression was profiled using Agilent SurePrint® microarrays. MicroRNA data were analyzed using Agilent GeneSpring® software, and TargetScan and WikiPathways were used to identify genes and pathways targeted by the differentially expressed miRNAs. Six miRNAs were differentially expressed in CSCs isolated from doxorubicin-sensitive cells, while fourteen miRNAs were differentially expressed in CSCs isolated from doxorubicin-resistant cells. The differentially expressed miRNAs in CSCs are associated with reduced proliferation and maintenance of the CSC phenotype, including drug resistance. Wnt signalling, EGFR1 signalling, Transforming Growth Factor (TGF)-beta receptor signalling, Toll-like receptor signalling and Type II interferon signalling (IFNG) were among the major pathways regulated by the dysregulated miRNAs in CSCs. These genes and pathways are involved in stem-cell maintenance, drug resistance and enhanced survival, making them potential therapeutic targets that warrant further study. This work identified miRNAs in drug-resistant CSCs that have not been previously linked to doxorubicin (or other drug) resistance in canine mammary tumour. Moreover, it identified miRNAs not previously characterized in cancer.

Keywords: cancer stem cell, canine mammary gland tumour, microarray, microRNA

[1]*Department of Veterinary Clinical Studies, Faculty of Veterinary Medicine, Universiti Putra Malaysia, 43400 UPM Serdang, Malaysia*

[2]*Department of Clinical Studies, Faculty of Veterinary Medicine, Universiti Malaysia Kelantan, Pengkalan Chepa 16100, Kota Bharu, Kelantan, Malaysia*

[3]*CanRes MAKNA Laboratory, Institute of Biosciences, Universiti Putra Malaysia, 43400 UPM Serdang, Malaysia*

[4]*Department of Veterinary Pre-clinical Sciences, Faculty of Veterinary Medicine, Universiti Putra Malaysia, 43400 UPM Serdang, Malaysia*

[5]*Department of Veterinary Laboratory Diagnostics, Faculty of Veterinary Medicine, Universiti Putra Malaysia, 43400 UPM Serdang, Malaysia*

[6]*Department of Biomedical Sciences, Faculty of Medicine and Health Sciences, Universiti Putra Malaysia, 43400 UPM Serdang, Malaysia*

***Correspondence**: gayathri@upm.edu.my* (G.T. Selvarajah)

Received August 15, 2025
Accepted January 19, 2026

Introduction

In 2006, The American Association for Cancer Research (AACR) defined Cancer Stem Cells (CSCs) as "*a cell within a tumor that possess the capacity to self-renew and to cause the heterogeneous lineages of cancer cells that comprise the tumor*" (Clarke *et al.*, 2006). Cancer Stem Cells, or cancer-initiating cells, are a subpopulation capable of initiating or repopulating tumours with differentiated cancer cells (Ouzounova *et al.*, 2013). CSCs comprise only about 0.1–4% of the cancer cell population but are responsible for metastasis and recurrence in many cancers (Louie *et al.*, 2010; Bao *et al.*, 2013). These characteristics result from CSC longevity, self-renewal, resistance to apoptosis, dormancy, and the ability to differentiate into tumour cells (Cocola *et al.*, 2009; Bao *et al.*, 2013). Additionally, CSCs express ATP-binding cassette (ABC) proteins and can actively efflux potentially harmful substances, including chemotherapeutic agents, conferring drug resistance (Begicevic and Falasca, 2017; Cho and Kim, 2020). Other mechanisms of CSC drug resistance include activation of cytoprotective pathways (such as NOTCH), robust DNA repair, alteration of drug targets, and a quiescent state (Mengistu *et al.*, 2024). Consequently, even after treatments that eliminate differentiated tumour cells, tumours frequently recur and may metastasize due to surviving drug-resistant, self-renewing CSCs. Therapeutic targeting of specific genes and pathways expressed in CSCs and drug-resistant CMT cells has reduced the CSC population and improved treatment sensitivity (Song *et al.*, 2013; Park *et al.*, 2014).

Gene expression studies in cancer, including CMT, report intra-tumour heterogeneity and differences in gene expression between cells within the same tumour (Turna *et al.*, 2023). This heterogeneity partly reflects differences between CSCs and differentiated tumour cells. CSCs express gene sets not necessarily present in the bulk tumour cells (Cocola *et al.*, 2009; Bao *et al.*, 2013), and these differences underline distinct phenotypes. Likewise, drug-resistant cancer cells express and activate genes and pathways that confer resistance (Sahabi *et al.*, 2022).

MicroRNAs (miRNAs) are 20–24 nucleotide non-coding RNAs that regulate translation of mRNAs into protein (Jansson and Lund, 2012). miRNA expressions and activity are conserved across vertebrates and invertebrates (Griffiths-Jones, 2010; Acunzo *et al.*, 2015). Post-transcriptional regulation by miRNAs is vital for cell proliferation, cell-cycle control, apoptosis, migration, differentiation, metabolism, and stem-cell maintenance in normal and cancerous cells (Jansson and Lund, 2012; Rothschild, 2014). Since their discovery approximately three decades ago, miRNAs have been attractive targets in oncology research (Ambros, 1989; Piva *et al.*, 2013; Song *et al.*, 2013; Zadran *et al.*, 2013; Schultz *et al.*, 2014; Tang *et al.*, 2016; Fish *et al.*, 2020), and several miRNAs have been modulated for therapeutic applications (Rothschild, 2014; Zhang *et al.*, 2015; Xu *et al.*, 2021). MiRNAs can act as tumour suppressors or oncogenes depending on their expression and activity (Qin *et al.*, 2013). The expression and dysregulation of miRNAs in human and canine cancers have been highlighted previously (Sahabi *et al.*, 2018), including roles in metastasis (miRNA-34a) and CSC propagation and patient survival (miRNA cluster 14q32). miRNAs also regulate ABC transporter expression, influencing drug resistance in cancers, including CSCs (Lu and Jin, 2024; Cho and Kim, 2020).

Doxorubicin is commonly used to treat CMT (Zambrano-Estrada *et al.*, 2018). It inhibits topoisomerase II, causing DNA damage and cell death (Johnson-Arbor and Dubey, 2023). Recently, miRNAs have been implicated in doxorubicin resistance by targeting ABC transporter expression in human cancers (Lu and Jin, 2024) and in CMT (Sahabi *et al.*, 2022).

Spontaneous CMTs have been proposed as large-animal models of human breast cancer, but relatively few studies have explored gene expression in putative CSCs and drug-resistant cells in CMT. More studies are needed to identify molecular markers and therapeutic targets in CMT CSCs, including those with acquired drug resistance. Differential miRNA expression in CMT stem-like cells was previously investigated (Rybicka *et al.*, 2015), but no study has yet examined differential miRNA expression in CSCs of drug-resistant CMT. Therefore, this study aimed to determine mRNA and miRNA expression, biological processes, and signaling pathways active in putative CMT CSCs with differing doxorubicin sensitivity.

Materials and Methods

Cell lines and culture conditions: In our previous work, a doxorubicin-resistant cell line (CMT-Star) was developed from a primary cell line (CMT-Stylo) established from a dog with CMT. CMT-Star demonstrated doxorubicin resistance, proliferating continuously in medium containing 100 nM doxorubicin (IC50 5013 nM) compared to CMT-Stylo (IC50 404.3 nM) by MTT assay. CMT-Star also showed reduced sensitivity to vincristine, cyclophosphamide, carboplatin and meloxicam (Sahabi *et al.*, 2022).

For the current work, CMT-Stylo cells were maintained in Dulbecco's Modified Eagle Medium (DMEM) supplemented with 10% fetal bovine serum (FBS) and 1% penicillin–streptomycin (Gibco™, USA) at 37°C in 5% CO2. CMT-Star cells were maintained with an additional 5 nM doxorubicin to preserve the resistant phenotype. The experimental workflow is summarized in Figure 1.

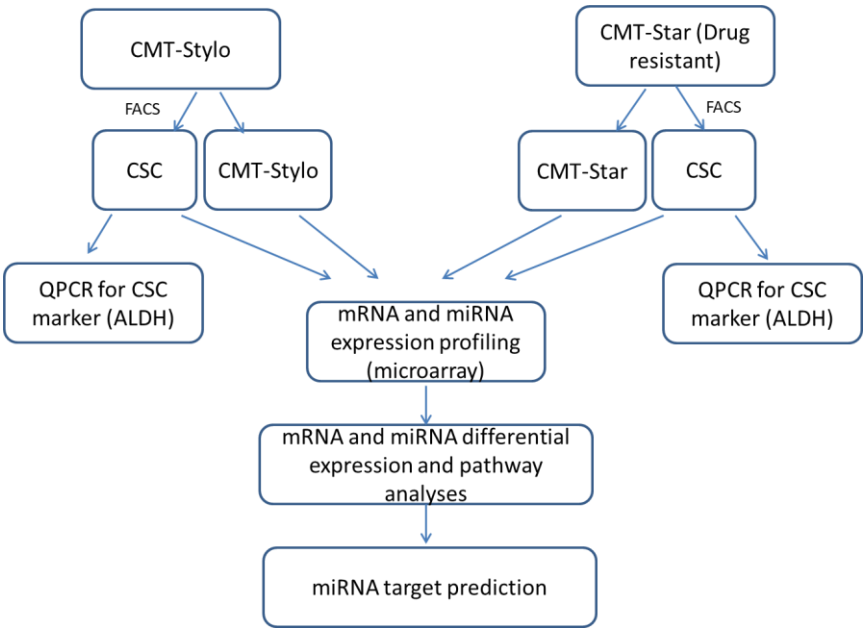

Figure 1 Flow chart presenting the major steps in the research design.

Fluorescence-activated cell sorting (FACS) for putative CSC isolation: Cells were dissociated with TrypLE™ Express (ThermoFisher Scientific, USA) to generate single-cell suspensions, passed through 40-µm cell strainers (BD Bioscience, USA), counted, and aliquoted. After centrifugation (2,000 rpm, 5 min), cells were resuspended in 100 µL PBS and incubated with antibodies (1 µL per 200,000 cells) for 1 h on ice in the dark. Phycoerythrin-conjugated CD24 (clone M1/69, BD Pharmingen™ USA) and allophycocyanin-conjugated CD44 (clone IM7, BD Pharmingen™ USA) were used. After washing, cells were resuspended in 500 µL PBS and sorted on a FACSAria III (BD Bioscience, USA). Acquisition and analysis used BD FACSDiva software v6.1.3. Post-sorting purity was determined. Putative CSCs were defined as CD44+ and CD24-/low (Al-Hajj *et al.*, 2003). These markers have been validated for CMT cells (Magalhães *et al.*, 2013; Im *et al.*, 2015). CD44 overexpression enhances self-renewal, proliferation, migration and metastasis (Calcagno *et al.*, 2010), while CD24 expression associates with differentiation (Rostoker *et al.*, 2016).

RNA isolation and cDNA synthesis: Total RNA was isolated from four populations: CMT-Stylo cells, CMT-Star cells, CMT-Stylo CSCs and CMT-Star CSCs (CSCs = CD44+ and CD24-/low) using the RNeasy Plus Mini Kit (Qiagen®, Germany) per manufacturer's instructions. Genomic DNA was removed with gDNA spin columns and an RNase-free DNase kit (Qiagen®). RNA concentration and purity were measured with an Infinite® 200 PRO NanoQuant spectrophotometer. One microgram of RNA from each sample was reverse transcribed to cDNA using the QuantiNova Reverse Transcription Kit (Qiagen®).

QPCR for ALDH expression in CSCs: ALDH expression was assessed by qPCR to confirm CSC identity, as previously reported for breast CSCs (Moreira *et al.*, 2018). ALDH is an established CSC marker (Im *et al.*, 2015) and validated in CMT CSCs (Michishita *et al.*, 2012). Quantification was normalized to TBP and RPS19 to determine fold change in CSCs relative to their respective cell lines. Primer sequences (validated in CMT) were as previously described (Michishita *et al.*, 2012; Tomiyasu *et al.*, 2010; Selvarajah *et al.*, 2009). Fifty nanograms cDNA per reaction were quantified using QuantiNova SYBR (Qiagen®) on a CFX96 Real-Time System (Bio-Rad®, USA) with three technical replicates per gene. Cycling began with a 2-min hot start at 95°C, followed by 40 cycles of 95°C (5 s) and gene-specific annealing/extension (15 s).

Gene expression profiling of CSCs and parent lines

Microarray hybridization, normalization and analysis: Small RNA quality was confirmed with RNA 6000 Nano/Small RNA kits and an Agilent 2100 Bioanalyzer. Samples with RIN ≥ 7 were hybridized in technical duplicates. Fifty nanograms per sample were Cy3-labelled using the One-Color Low Input Quick Amp Labelling Kit (Agilent). Cy3-labelled cRNA was fragmented and hybridized (in duplicate) to Agilent SurePrint Canine Gene Expression 4×44K Microarray v2 (Design ID: 021193) for 17 h at 65°C. Slides were washed and scanned on an Agilent SureScan® Microarray Scanner (G4900DA) at 5-µm resolution (532 nm). Feature Extraction software provided normalized intensities for further analysis.

Agilent GeneSpring Analysis Software v14.8 (default flag settings) was used for detection calls. Signal intensities were normalized to the 90th percentile with baseline transformation to the median of all samples. Hierarchical clustering of differentially expressed genes was performed.

Microarray validation: Selected differentially expressed genes (two upregulated, two downregulated) were validated by qPCR. Validation assessed direction of expression and fold change concordance between microarray and qPCR. Primers were canine-specific; see Table 1 for sequences and annealing temperatures.

Pathway analysis: Pathway enrichment used a single experiment analysis (SEA)-moderated t-test. For pathway selection, genes were filtered by P-value and fold change ($P < 0.01$ and fold change ≥ 10 for CMT-Stylo vs. CMT-Stylo CSCs; $P < 0.05$ for CMT-Star vs. CMT-Star CSCs). DAVID was used for gene ontology to identify biological processes, molecular functions and cellular components. Venn diagrams (Venny v2.1.0, Oliveros, J.C., 2015) compared regulated pathways between CMT-Star and CMT-Stylo CSCs.

miRNA profiling: Four RNA samples were normalized to 100 ng and Cy3-labelled using the miRNA Complete Labeling and Hyb Kit (Agilent). Samples were fragmented and hybridized (in duplicate) to Agilent SurePrint® G3 Custom miRNA 8×60K (Design ID: 084492) at 55°C for 20 h. Slides were washed and scanned on an Agilent SureScan® Scanner (G4900DA) at 3-µm resolution. Normalized intensities were extracted with Agilent Feature Extraction software (v11.5.1.1). miRNA microarray data were deposited in GEO under accession GSE114889.

Table 1 Genes and primer sequences used for microarray result QPCR validation.

Gene	Primers	Tm	Accession number/Reference
Interleukin 6	F (5′-CTCTCCACAAGCGCCTTCTC-3′)	60⁰C	(Peters *et al.*, 2005)
	R (5′-TGAAGTGGCATCATCCTTGG-3′)		
MXD-1	F (5′- TGGAGGCTCTGTCAGGAGTT -3′)	60⁰C	NM_001003134
	R (5′- TTGCCTTCAGTCCCTCTGTC-3′)		
GAPDH	F (5′-TGTCCCCACCCCCAATGTATC-3′)	58⁰C	NM_001003142
	R (5′-CTCCGATGCCTGCTTCACTACCTT3′)		

GAPDH is the reference gene

Differential miRNA expression analysis: Microarray data were analyzed in Agilent GeneSpring® v14.8. A moderated t-test with Benjamini–Hochberg FDR was used, with $P \leq 0.05$ and fold change ≥ 2. Volcano plots visualized fold change against significance. Bonferroni family-wise error rate (FWER) at $P < 0.05$ and fold change ≥ 2 was also applied (Fu *et al.*, 2014).

Target prediction and pathway assignment: TargetScan was used to predict mRNAs targeted by differentially expressed miRNAs. Pathway analysis of targeted genes used SEA-moderated t-test with Selected Annotations (RefSeq Protein ID, Entrez Gene ID, Ensembl Gene ID, GenBank Accession, UniGene ID, TIGR ID) and Selected Pathway Source (WikiPathways) for *Canis lupus familiaris*.

Comparisons and statistics: Venn diagrams compared dysregulated miRNAs, targeted genes and pathways (Venny v2.1.0). qPCR data were analyzed by the ΔΔCt method using CFX Manager v3.1 (Bio-Rad®) and presented as fold change; significance was set at $P < 0.05$. Microarray differential expression used a moderated t-test with Benjamini–Hochberg FDR (Yu *et al.*, 2011); Bonferroni FWER was also explored.

Results

CSCs isolated by flow cytometry: Both CMT-Stylo and CMT-Star populations contained CD44+ / CD24-/low CSCs (Figs 2a and 2b). CMT-Stylo CSCs comprised 2.8% (~2,790 cells) of 5,000,000 total cells in the sorting tube; CMT-Star CSCs comprised 7.6% (~7,540 cells). Post-sorting purity was 93% for CMT-Stylo CSCs and 91% for CMT-Star CSCs.

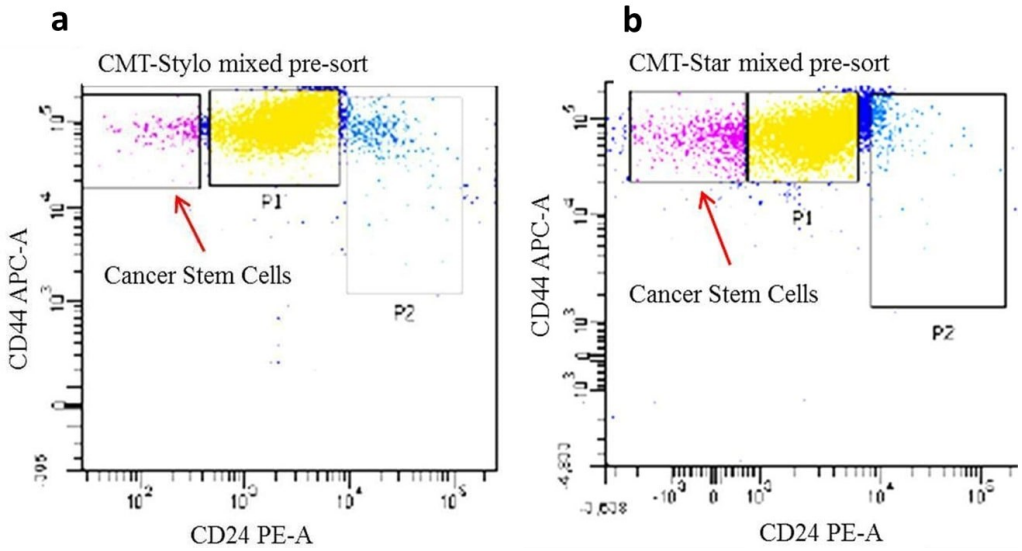

Figure 2 FACS gating for isolating CSCs from CMT-Stylo cells (a) and CMT-Star cells (b).
Legend: Gating of the target cells was done to exclude doublets and debris to ensure high purity of the sorted cells from CMT-Stylo cells. The total events in singlet 2 were 10,000 events (cells). For CMT-Star cells. The total events in singlet 2 were 9,974 events (cells). Cancer stem cells with CD44+ and CD24-/low phenotype were sorted from both cell groups.

ALDH expression in canine mammary CSCs: Aldehyde dehydrogenase expression was 9-fold higher in CMT-Stylo CSCs and 3-fold higher in CMT-Star CSCs compared to their respective parent lines (ANOVA, $P < 0.05$), supporting successful CSC isolation.

Gene expression normalization and clustering: Of 43,663 detected entities, 43,620 remained after normalization. Hierarchical clustering showed a distinct expression profile for CMT-Stylo cells compared to other samples. Gene expression data were deposited in GEO under accession GSE114888.

Differential gene expression in CMT-Stylo CSCs: Using $P < 0.01$ and absolute fold change ≥ 10 (Benjamini–Hochberg), 508 entities were differentially expressed in CMT-Stylo CSCs versus CMT-Stylo cells (145 unknown ESTs; 54 not functionally annotated for dog) (Supplemental material 1). For this comparison, the threshold (*P*-value and fold change) choice was driven by data distribution and multiple-testing considerations, and biological relevance was still considered despite statistical stringency. Table 2 lists pathways regulated by these genes. Figures 3 and 4 show hierarchical clustering and a volcano plot for $P < 0.01$ and fold change ≥ 10 (Benjamini–Hochberg moderated t-test).

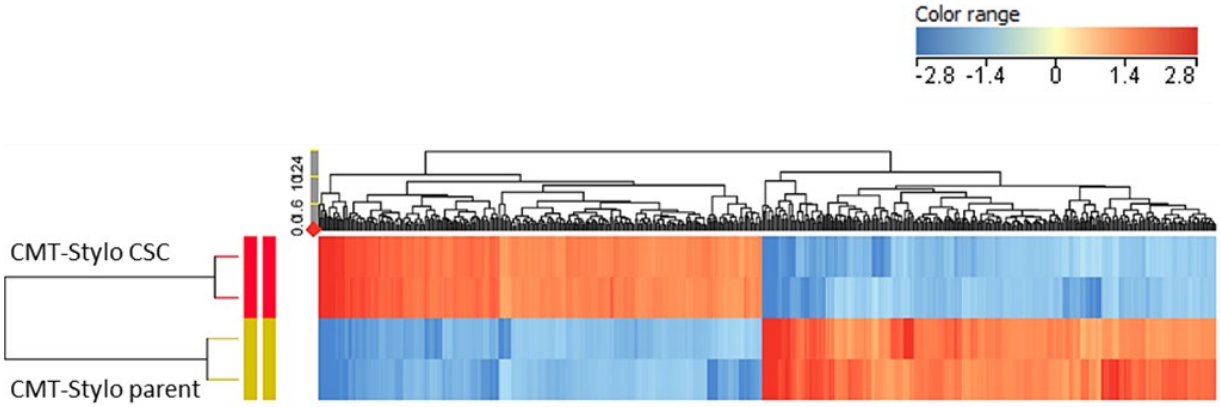

Figure 3 Hierarchical clustering (dendrogram) based on 508 entities differentially expressed entities: 251 up regulated and 257 down regulated in duplicate samples of CSC isolated from CMT-Stylo cells compared to CMT-Stylo cells.
Legend: The technical replicates of each sample (CMT-Stylo CSC and the CMT-Stylo cells) demonstrated similar pattern of gene/entities expression by clustering together.

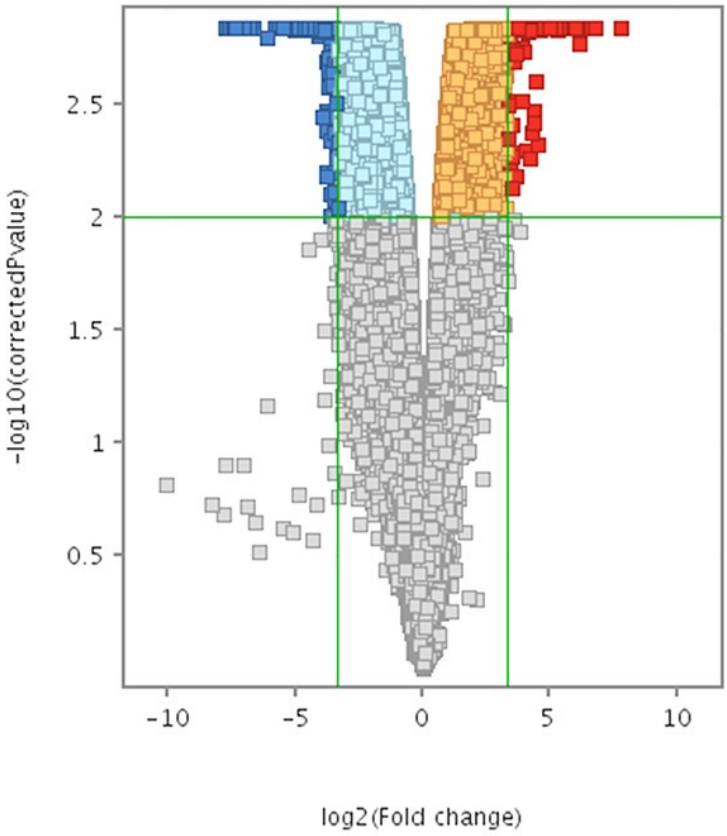

Figure 4 Volcano plots of differentially expressed entities between CMT-Stylo CSC and CMT-Stylo cells.
Legend: Entities with different expression in CSC compared to CMT-Stylo cells at $P < 0.01$ (y-axis) and absolute fold change of 10 (x-axis) (Benjamini Hochberg moderated t-test). Blue colored entities are down regulated while the red colored entities are up regulated in the CSC. The pale blue, orange and grey-colored entities did not fall within the cut-off values set for the analysis.

Table 2 Pathways with a minimum of 2% matched entities out of the 54 pathways regulated in CMT-Stylo CSC compared to CMT-Stylo cells.

Pathway	p-value	Matched Entities	Gene	Pathway Entities	% matched
Blood Clotting Cascade	0.0171	2	PLAU, PLG	17	11.76
Cytokines and Inflammatory Response	0.03036	2	IL6, CSF2	24	8.33
Nuclear Receptors	0.00896	3	NR2F1, NR4A1, NR4A2	38	7.89
Oxidative Stress	0.03287	2	NFIX, FOS	26	7.69
Endochondral Ossification	0.00276	4	PTHLH, DDR2, PLAU, ALPL	56	7.14
Adipogenesis	0.00128	6	LOC483120, IL6, BMP2, FZD1, NR2F1, EBF1	123	4.88
Toll-like receptor signalling pathway	0.01081	4	FOS, IL6, CCL5, TLR2	84	4.76
Complement and Coagulation Cascades	0.09291	2	PLAU, PLG	47	4.26
Transforming Growth Factor (TGF)Beta Signalling	0.08567	2	TGFBR3, FOS	47	4.26
Wnt Signalling Pathway	0.01816	4	ROR2, LRP1, FZD1, CDH1,	101	3.96
Metapathway biotransformation	0.00824	5	Q2VB21_CANFA, CYP26B1, GSTO1, GSTO2, HS3ST3B1	133	3.76
IL-6SignallingPathway	0.07908	3	IL6, BTK, FOS	95	3.16
Wnt Signalling Pathway and Pluripotency	0.20728	2	FZD1, PLAU	86	2.33
Integrin-mediated cell adhesion	0.24674	2	CAPN5, ITGAE	92	2.17

Gene ontology: Upregulated genes in CMT-Stylo CSCs were enriched for processes including positive regulation of interleukin-6 production, negative regulation of canonical Wnt signalling, negative regulation of cell cycle, positive regulation of sequence-specific DNA binding, MAPK cascade, cell migration, positive regulation of apoptosis, and negative regulation of cell proliferation. Supplemental material 2 summarizes molecular functions, biological processes and cellular components for up- and down-regulated genes.

Differential gene expression in CMT-Star CSCs: With $P < 0.05$ and absolute fold change ≥ 5 (Benjamini–Hochberg), 306 entities were differentially expressed in CMT-Star CSCs versus CMT-Star cells (83 unknown ESTs; 17 not functionally annotated) (Supplemental material 3). Table 3 lists regulated pathways. Figures 5 and 6 show clustering and a volcano plot for $P < 0.05$ and fold change ≥ 5 (Benjamini–Hochberg moderated t-test).

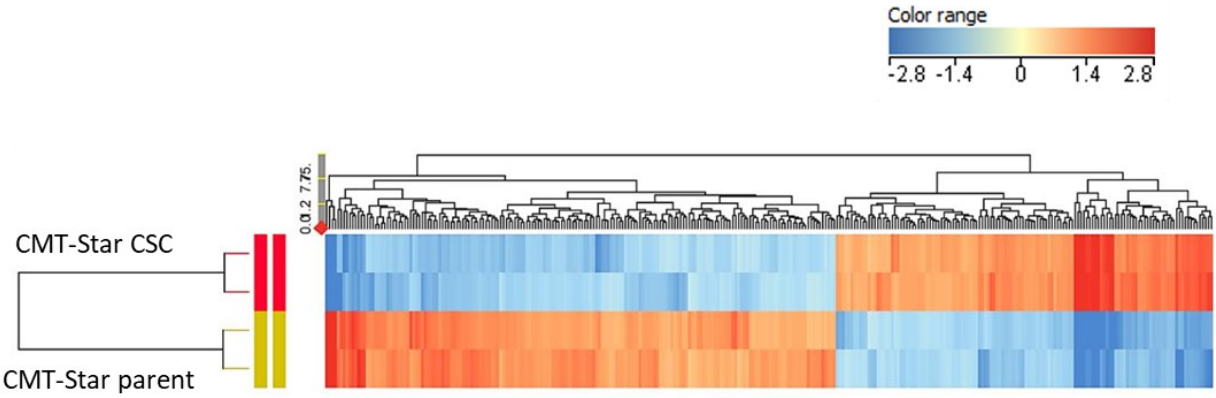

Figure 5 Hierarchical clustering (dendrogram) of 306 differentially expressed entities: 130 up regulated and 176 down regulated in duplicate samples of CSC isolated from CMT-Star cells compared to CMT-Star cells.
Legend: The technical replicates of each sample (CMT-Star CSC and the CMT-Star cells) demonstrated similar pattern of gene/entities expression by clustering together.

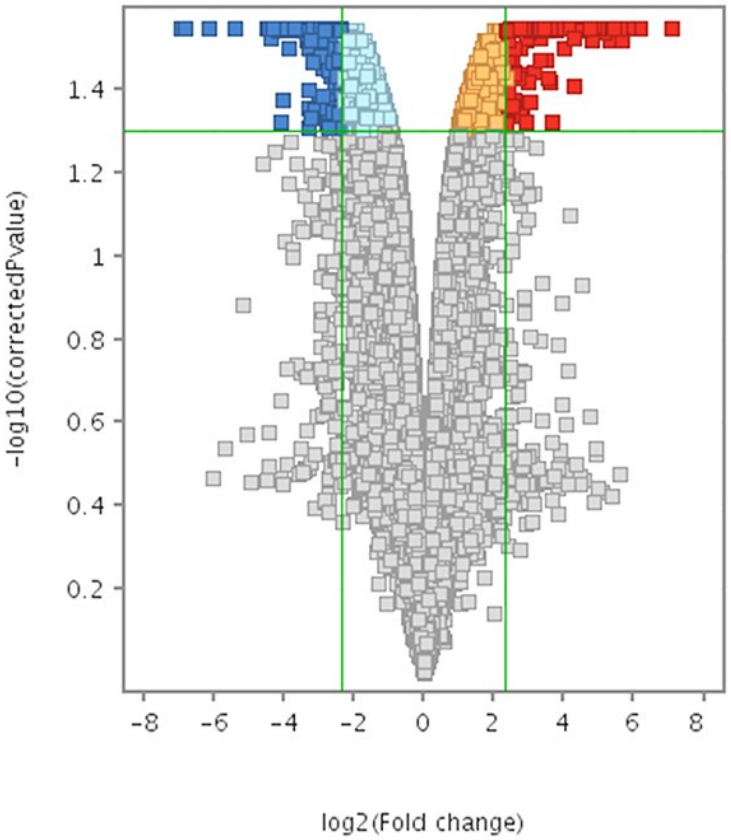

Figure 6 Volcano plots of the differentially expressed entities between CMT-Star CSC and CMT-Star cells
Legend: Entities with different expression in CMT-Star CSC compared to CMT-Star cells at $P < 0.05$ (y-axis) and absolute fold change of 5 (x-axis) (Benjamini Hochberg moderated t-test). Blue colored entities are down regulated while the red colored entities are up regulated in the CSCs. The pale blue, orange and grey-colored entities did not fall within the cut-off values set for the analysis.

Table 3 Pathways (with minimum of 2 matched entities) of the 36 pathways regulated in CMT-Star CSC compared to CMT-Star cells.

Pathway	p-value	Matched Entities	Gene	Pathway Entities	% matched
Cytokines and Inflammatory Response	2.14E-05	4	IL6, IL4, DLA-DRB1, DLA-DRA1	24	16.67
Inflammatory Response Pathway	0.001193	3	THBS1, IL4, CD86	30	10.00
Type II interferon signalling (IFNG)	0.0010753	3	PSMB9, IFIT2, LOC478170	31	9.68
Oxidative Stress	0.0129728	2	MGST1, XDH	26	7.69
Matrix Metalloproteinases	0.0119483	2	MMP16, MMP1	27	7.41
Complement and Coagulation Cascades	0.0037396	3	SERPINC1, SERPINA5, SERPINE1	47	6.38
Striated Muscle Contraction	0.0224474	2	ACTC1, ACTA2	35	5.71
Transforming Growth Factor (TGF) Beta Signalling Pathway	0.0355713	2	THBS1, SERPINE1	47	4.26
Proteasome Degradation	0.0473538	2	PSMB9, PSMB8	53	3.77
Toll-like receptor signalling pathway	0.0155039	3	CD86, IL6, CCL5	84	3.57
IL-4signalling Pathway	0.0509478	2	IL4, IL13RA1	57	3.51
Adipogenesis	0.036311	3	SREBF1, SERPINE1, IL6	123	2.44
Androgen receptor signalling pathway	0.091542	2	ROCK1, PIAS1	82	2.44
Integrin-mediated cell adhesion	0.1144043	2	RAC2, ROCK1,	92	2.17
Calcium Regulation in the Cardiac Cell	0.0626973	3	ATP2A3, SLC8A1, GJB1	141	2.13
Transforming Growth Factor(TGF) Beta Receptor Signalling Pathway	0.0615084	3	ROCK1, PIAS1, ACVRL1	146	2.05

Gene ontology: Upregulated genes in CMT-Star CSCs were enriched for immune response and cellular response to tumor necrosis factor. Supplemental material 4 summarizes gene ontology results.

Microarray validation: qPCR validated selected genes: IL6 was upregulated by 3.5- and 3.0-fold (microarray) in CMT-Stylo CSCs and CMT-Star cells, respectively; qPCR showed 3.9- and 2.2-fold upregulation. MX1 was upregulated by 3.7- and 2.2-fold (microarray and qPCR, respectively) in CMT-Star CSCs versus CMT-Star cells. Small discrepancies may reflect qPCR sensitivity and microarray detection of transcript variants; directions of change were concordant.

Differential miRNA expression: After normalization and filtering, 425 entities remained for analysis.

CMT-Stylo CSCs: A moderated t-test (Benjamini–Hochberg FDR; $P \leq 0.05$; fold change ≥ 2) identified six differentially expressed miRNAs (Fig. 7; Table 4): four upregulated and two downregulated in CSCs versus CMT-Stylo cells. Bonferroni FWER also supported dysregulation of these six miRNAs. Target prediction yielded 154 MIMAT accession numbers (Supplemental material 5).

Table 5 lists pathways regulated by mRNAs targeted by these miRNAs.

A Venn diagram comparing dysregulated mRNAs (from gene expression) and mRNAs targeted by dysregulated miRNAs in CMT-Stylo CSCs revealed three common genes: upregulated GBF1 and FBXO31, and downregulated CALML5. Eight common pathways were shared (Fig. 8): Endochondral Ossification; Toll-like receptor signalling; Wnt signalling Pathway NetPath; MAPK signalling; Insulin signalling; EGFR1 signalling; Regulation of Actin Cytoskeleton; and TGF-beta receptor signalling.

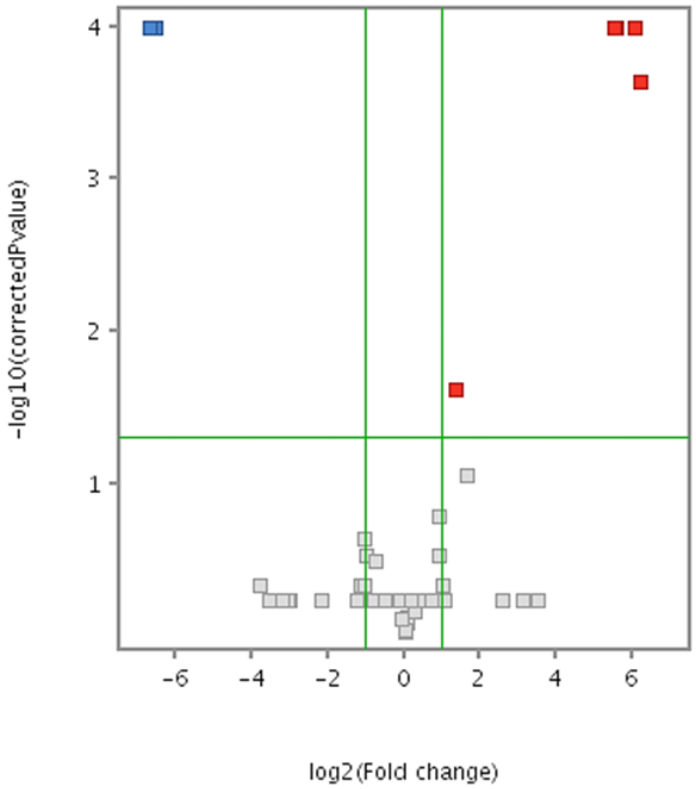

Figure 7 Volcano plot of differentially transcribed entities (miRNAs) in CMT-Stylo CSC compared to CMT-Stylo cells.
Legend: Six entities (miRNAs) differentially transcribed in CMT-Stylo CSC (with Benjamini-Hochberg FDR method) at $P < 0.05$(y-axis) and fold change cut off at 2.0 (x-axis). Blue colored entities are downregulated while the red colored entities are upregulated in the CSC. The grey-colored entities did not fall within the cut-off values set for the analysis.

Table 4 Dysregulated microRNAs in CMT-Stylo CSC compared to the CMT-Stylo cells.

Systematic name	*p* value	Regulation	Fold change	Log Fold change
cfa-miR-8815	3.21E-06	Up	74.015	6.209
cfa-miR-93	1.47E-07	Up	65.346	6.030
cfa-miR-874	4.65E-09	Up	47.083	5.557
cfa-miR-99b	8.39E-09	Up	44.876	5.4878
cfa-miR-483	2.19E-09	Down	-91.625	-6.517
cfa-miR-8816	1.76E-09	Down	-103.667	-6.695

All the miRNAs were differentially expressed based on Bonferroni correction at $p < 0.05$ and FC of 2.0.

Table 5 Pathways with a minimum of two matched entities regulated by genes targeted by the dysregulated microRNAs in CMT-Stylo CSC compared with CMT-Stylo cells.

Pathway	p-value	Matched Entities	Pathway Entities
Insulin Signaling	3.01E-12	5	155
MAPK signaling pathway	1.25E-07	3	151
Transforming Growth Factor (TGF) Beta Receptor Signaling Pathway	1.25E-07	3	146
Calcium Regulation in the Cardiac Cell	2.51E-05	2	141
EGFR1Signaling pathway	2.51E-05	2	165
Biogenic Amine Synthesis	2.51E-05	2	13
mRNA processing	2.51E-05	2	119
Toll-like receptor signaling pathway	2.51E-05	2	84
Osteoblast	2.51E-05	2	13
Alpha6-Beta4IntegrinSignalingPathway	2.51E-05	2	64
Regulation of Actin Cytoskeleton	2.51E-05	2	137
Wnt Signaling Pathway	2.51E-05	2	101
Endochondral Ossification	2.51E-05	2	56

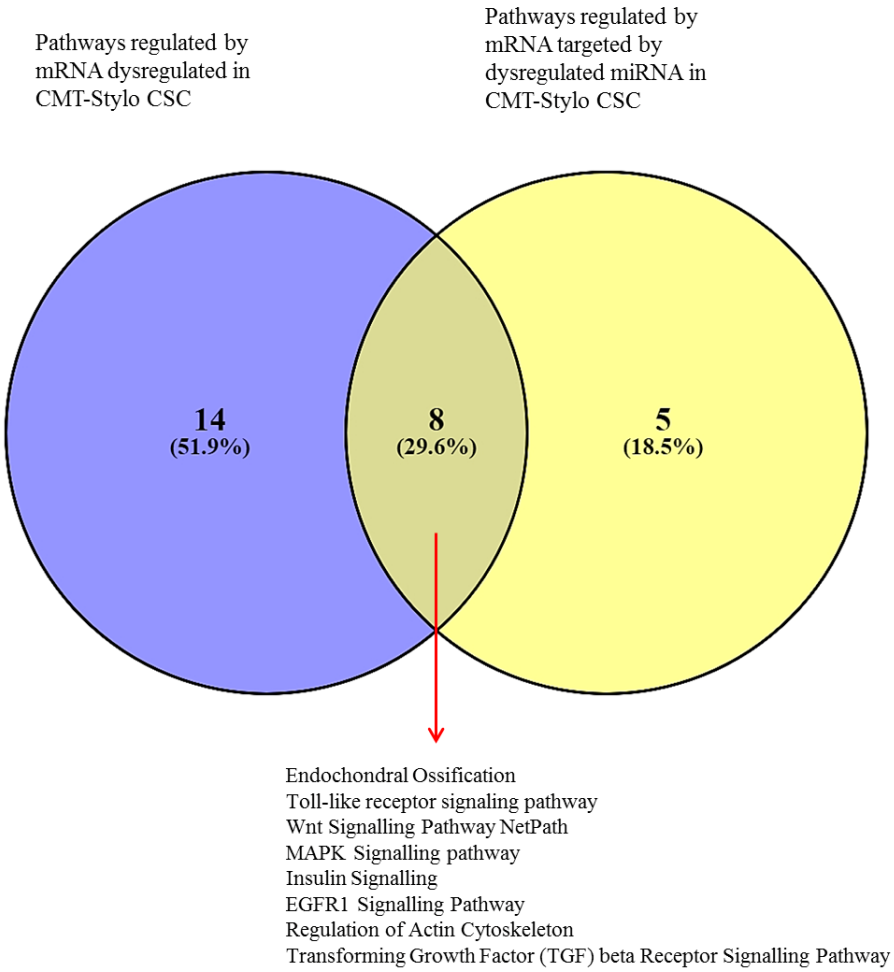

Figure 8 Venn diagram of common pathways regulated by mRNAs dysregulated in CMT-Stylo CSCs (from the gene expression study) and mRNAs targeted by dysregulated miRNAs in CMT-Stylo CSCs.
Legend: Eight pathways regulated in CSC of CMT-Stylo cells are shown at the intercept of the Venn diagram; Endochondral Ossification, Toll-like receptor signaling pathway, Wnt signalling Pathway NetPath, MAPK signalling pathway, Insulin signalling, EGFR1 signalling Pathway, Regulation of Actin Cytoskeleton and Transforming Growth Factor (TGF) beta Receptor signalling Pathway.

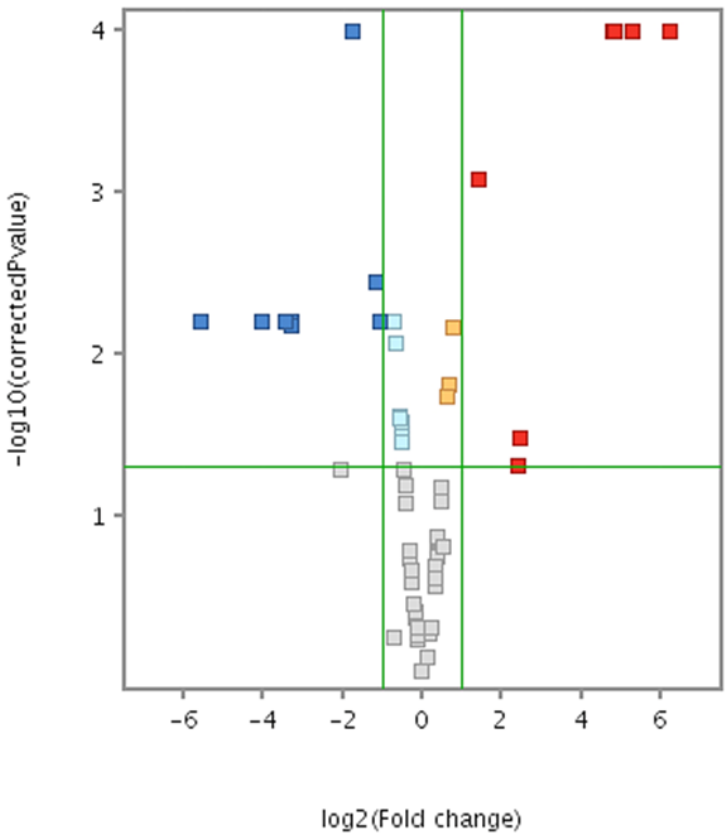

Figure 9 Volcano plot of differentially transcribed entities (microRNAs) in CMT-Star CSC compared to CMT-Star cells.
Legend: Fourteen entities (miRNAs) transcribed in CMT-Star CSC compared to CMT-Star cells (with Benjamini-Hochberg FDR method) at P <0.05 (y-axis) and fold change cut off at 2.0 (x-axis). Blue colored entities are downregulated, while the red colored entities are upregulated in the CSC. The pale blue, orange and grey-colored entities did not fall within the cut-off values set for the analysis.

Table 6 Dysregulated microRNAs in CMT-Star CSC compared to CMT-Star cells.

Systematic name	p value	Regulation	Fold change	Log Fold change
***cfa-miR-31**	**4.79E-16**	**Up**	**71.867**	**6.167**
***cfa-miR-151**	**1.22E-14**	**Up**	**37.996**	**5.247**
***cfa-miR-183**	**1.13E-12**	**Up**	**28.108**	**4.812**
***cfa-miR-106a**	**4.85E-14**	**Up**	**26.713**	**4.739**
cfa-miR-8816	0.029955	Up	5.294	2.404
cfa-miR-8833	4.38E-02	Up	5.176	2.372
***cfa-miR-92a**	**1.16E-05**	**Up**	**2.577**	**1.366**
cfa-miR-125b	3.15E-04	Down	-2.038	-1.027
***cfa-miR-29a**	**5.93E-05**	**Down**	**-2.303**	**-1.203**
***cfa-miR-22**	**6.01E-07**	**Down**	**-3.385**	**-1.759**
cfa-miR-155	0.001684	Down	-9.809	-3.294
cfa-miR-8794	5.83E-03	Down	-10.103	-3.336
cfa-miR-8803	1.11E-03	Down	-11.047	-3.465
cfa-miR-149	3.36E-04	Down	-16.816	-4.071

*Differentially expressed based on Bonferroni correction at $p < 0.05$ and FC of 2.0.

Table 7 Pathways with a minimum of two matched entities regulated by genes targeted by the dysregulated microRNAs in CMT-Star CSC compared with CMT-Star cells.

Pathway	p-value	Matched Entities	Pathway Entities
MAPK signaling pathway	3.18E-15	7	151
T Cell Receptor Signaling Pathway	4.50E-11	5	119
TNF-alpha NF-kB Signaling Pathway	4.50E-11	5	170
Insulin Signaling	4.50E-11	5	155
B Cell Receptor Signaling Pathway	4.50E-11	5	147
Calcium Regulation in the Cardiac Cell	5.32E-09	4	141
EGFR1Signaling Pathway	5.32E-09	4	165
GPCRs Class A Rhodopsin-like	5.32E-09	4	195
IL-5 Signaling Pathway	5.32E-09	4	62
G Protein Signaling Pathways	6.26E-07	3	82
IL-2 Signaling Pathway	6.26E-07	3	72
Complement and Coagulation Cascades	6.26E-07	3	47
Type II interferon signaling (IFNG)	6.26E-07	3	31
IL-3 Signaling Pathway	6.26E-07	3	94
Triacylglyceride Synthesis	6.26E-07	3	22
Regulation of Actin Cytoskeleton	6.26E-07	3	137
Transforming Growth Factor (TGF) Beta Signaling Pathway	6.26E-07	3	47
Cytokines and Inflammatory Response	7.35E-05	2	24
Androgen receptor signaling pathway	7.35E-05	2	82
Notch Signaling Pathway	7.35E-05	2	44
Inhibitor of DNA Signaling Pathway	7.35E-05	2	45
FAS pathway and Stress induction of HSP regulation	7.35E-05	2	34
mRNA processing	7.35E-05	2	119
Toll-like receptor signaling pathway	7.35E-05	2	84
IL-6SignalingPathway	7.35E-05	2	95
Apoptosis	7.35E-05	2	71
IL-9SignalingPathway	7.35E-05	2	23
Hypertrophy Model	7.35E-05	2	19
Alpha6-Beta4IntegrinSignalingPathway	7.35E-05	2	64
Peptide GPCRs	7.35E-05	2	66
Transforming Growth Factor (TGF) beta Receptor Signaling Pathway	7.35E-05	2	146
Selenium metabolism Selenoproteins	7.35E-05	2	42
Meta pathway biotransformation	7.35E-05	2	133
EBV_LMP1_signaling	7.35E-05	2	23

Figure 10 Venn diagram of common pathways regulated by mRNAs dysregulated in CMT-Star CSCs (from the gene expression study) and mRNAs targeted by dysregulated miRNAs in CMT-Star CSCs.
Legend: Eleven pathways regulated in CSC of CMT-Star cells from both mRNA and miRNA results as shown at the intercept of the Venn diagram; Cytokines and Inflammatory Response, Calcium Regulation in the Cardiac Cell, Toll-like receptor signalling pathway, Complement and Coagulation Cascades, Type II interferon signalling (IFNG), Transforming Growth Factor (TGF) beta Receptor signalling Pathway, Androgen receptor signalling pathway, Metapathway biotransformation, Regulation of Actin Cytoskeleton and Transforming Growth Factor (TGF) Beta signalling Pathway.

CMT-Star CSCs: Fourteen differentially expressed miRNAs were identified by Benjamini–Hochberg FDR ($P \leq 0.05$; fold change ≥ 2), with seven upregulated and seven downregulated in CSCs versus CMT-Star cells (Fig. 9; Table 6). Bonferroni FWER identified seven miRNAs as significant ($P < 0.05$; fold change ≥ 2). Target prediction returned 263 MIMAT accession numbers (Supplemental material 6).

Table 7 shows the pathways regulated by the mRNAs targeted by the dysregulated miRNAs in CMT-Star CSCs.

A Venn diagram comparing dysregulated mRNAs and mRNAs targeted by dysregulated miRNAs in CMT-Star CSCs revealed four common genes: upregulated HERC5, IFI44L and LOC486400 (gamma-glutamyltransferase 1); and downregulated TAGLN. Eleven common pathways were shared (Fig. 10), including Cytokines and Inflammatory Response; Calcium Regulation in the Cardiac Cell; Toll-like receptor signalling; Complement and Coagulation Cascades; Type II interferon signalling (IFNG); TGF-beta receptor signalling; Androgen receptor signalling; Metapathway biotransformation; Regulation of Actin Cytoskeleton; and TGF-beta signalling.

Uncharacterized miRNAs: Five uncharacterized miRNAs were differentially expressed: miRNA-8803 (MIMAT0034293), miRNA-8815 (MIMAT0034305), miRNA-8816 (MIMAT0034306), miRNA-8833 (MIMAT0034326) and miRNA-8794 (MIMAT0034284). Literature searches returned only miRBase accessions; their roles in drug resistance and CSC phenotype require further investigation

Discussion

Cancer Stem Cells were isolated from CMT-Stylo and CMT-Star cells using established markers CD44 and CD24 and confirmed by ALDH expression. CMT-Star cells contained a higher proportion of CSCs than CMT-Stylo cells. Prior studies suggest drug-resistant CMT cells have higher CSC proportions (Zhou *et al.*, 2018), and exposure to chemotherapeutics (e.g., doxorubicin, 5-fluorouracil) can increase CSC marker expression and spheroid formation in human breast

and colorectal cancer models (Chong *et al.*, 2022; Babajnai *et al.*, 2025). Doxorubicin exposure can induce metabolic reprogramming toward a CSC-like, invasive, drug-resistant phenotype (Chong *et al.*, 2022). Our findings corroborate these reports: drug-resistant CMT-Star cells exhibited higher CSC numbers, and metabolic pathways were altered between CSCs and parent cells, supporting the use of CMT-Star cells for identifying therapeutic targets and screening agents.

Due to the scarcity of data on miRNA expressions in CMT CSC, additional very relevant data from human studies is cautiously referred to here. Upregulated genes in CMT-Stylo CSCs are involved in stem-cell maintenance, self-renewal, tumourigenicity, drug resistance and immune evasion, and many have been reported in other CSCs. IL33, IL6 and NR4A2 contribute to tumourigenicity, drug resistance and proliferation (Hou *et al.*, 2015; Fang *et al.*, 2017). TGFβR3 signalling and prostaglandin E synthase are linked to proliferation, drug resistance and tumourigenesis (Finetti *et al.*, 2015; Janakiram *et al.*, 2017). These genes, especially TGFBR and interleukins implicated in CSC biology, merit further exploration as markers of aggressive tumours and therapeutic targets.

Pathways regulated in CMT-Stylo CSCs include IL6 (associated with CSC propagation) (Berger *et al.*, 2023), IL5 and TNF-α (involved in immunomodulation) (Kang *et al.*, 2023), NF-κB (implicated in oncogenesis and apoptosis prevention) (Kaltschmidt *et al.*, 2019), EGFR (associated with self-renewal, drug resistance, metastasis) (Zhao *et al.*, 2020), TGF-β and TGFβR (involved in tumourigenicity) (Tang *et al.*, 2007; Jovanović *et al.*, 2014), Wnt signalling and pluripotency (associated with stemness and metastasis) (Yue *et al.*, 2018), and MAPK signalling (implicated in metastasis and drug resistance) (Kudaravalli *et al.*, 2022). Dysregulated miRNAs implicated in drug resistance and tumour progression include miRNA-93, miRNA-483, miRNA-874 and miRNA-99b (Hussen *et al.*, 2023; Liu *et al.*, 2020; Pan *et al.*, 2021; Niture *et al.*, 2023; Jiang *et al.*, 2022). To our knowledge, this is the first report implicating these miRNAs in CSCs isolated from CMT. Their expression warrants investigation as molecular markers and therapeutic targets. Although this study did not perform any functional studies on the genes and pathways dysregulated in these CSC, most have been implicated in tumour initiation and progression, including metastasis in different cancer types.

Differentially expressed genes in CMT-Star CSCs also support stem-cell maintenance, with additional genes enhancing resistance to cytotoxic agents. Because differentiated tumour cells derive from CSCs, drug-resistance genes may be maintained in the bulk tumour, explaining limited differences between CMT-Star CSCs and parent cells. Continuous culture of CMT-Star cells in 5 nM doxorubicin sustained expression of resistance genes, resulting in similar regulation across CSCs and parent cells. Upregulated genes such as xanthine dehydrogenase, IL6 and EPSTI1, and downregulated genes such as TNC and ROCK1, collectively maintain the CSC phenotype. Thus, dysregulated genes in CMT-Star populations support CSC maintenance while enabling differentiated tumour cells to acquire a somewhat more invasive and proliferative phenotype. The coexistence of CSCs and differentiated cells with distinct phenotypes emphasizes the importance of identifying therapeutic targets that can eradicate both populations.

Regulated pathways in CMT-Star CSCs—MMP, IL4 signalling, TGF-β, TGFβR and Wnt/β-catenin—are associated with stem-cell maintenance and enhanced drug resistance, consistent with CSCs from drug-resistant lines. Dysregulated miRNAs in these CSCs (e.g., miRNA-31, miRNA-151, miRNA-183, miRNA-106a, miRNA-125, miRNA-29a, miRNA-22, miRNA-155 and miRNA-149) were linked to these pathways. To our knowledge, this is the first report linking these miRNAs to drug resistance in canine mammary tumours; their dysregulation suggests roles in maintaining stem-cell traits, drug resistance, invasion and progression.

Five uncharacterized miRNAs identified here may have novel roles in CSC biology and drug resistance. The principal difference highlighted between CSCs and parent lines is the low proliferative yet self-renewing nature of CSCs. Uncharacterized miRNAs may associate with these properties. Further research is required to determine their specific roles in CSC biology and drug resistance.

In conclusion, several genes and pathways—including those regulated by differentially expressed miRNAs such as TGFβR, IL6, MAPK, nuclear receptors, Wnt signalling, TGF-β, TNF-α, EGFR1 and Notch—contribute to maintenance of the CSC phenotype, drug resistance and enhanced survival. This study identified miRNAs in drug-resistant CSCs not previously linked to doxorubicin (or other drug) resistance in CMT and miRNAs not yet characterized in cancer. Further functional studies using RNAi, ectopic expression, western blots, additional in-vitro assays and in-vivo models are necessary to establish the roles of these miRNAs and genes as molecular markers and therapeutic targets in CMT.

Conflicts of interest: The authors declare that they have no competing interests.

Acknowledgements

This research was primarily funded by the Ministry of Higher Education of Malaysia for Universiti Putra Malaysia through the Transdisciplinary Research Grant Scheme (TRGS/1/2014/UPM/02/6/3) with the vot number 5535001. The authors are thankful to the Faculty of Veterinary Medicine laboratory staff that assisted in the various procedures for this research (Post-Mortem, Clinical, Pharmacology and Biochemistry). A special appreciation is extended to Prof. Dr. Norjahan Banu Mohamed Alith-een for her kind support with flow cytometry assays, Miss Jovene for technical support in gene expression studies.

References

Acunzo M, Romano G, Wernicke D and Croce CM 2015. MicroRNA and cancer--a brief overview. Adv Biol Regul. 57: 1–9.

Al-Hajj M, Wicha MS, Benito-Hernandez A, Morrison SJ and Clarke MF 2003. Prospective identification of tumorigenic breast cancer cells. Proc Natl Acad Sci U S A. 100(7): 3983–3988.

Ambros V 1989. A hierarchy of regulatory genes controls a larva-to-adult developmental switch in *C. elegans*. Cell 57(1): 49–57.

Babajnai A, Rahmani S, Asadi MJ, Gheytanchi E and Adibhesami G 2025. Molecular and phenotypic characterization of 5-FU resistant colorectal cancer cells: toward enrichment of cancer stem cells. Cancer Cell Int. 25: 154.

Bao B, Ahmad A, Azmi AS, Ali S and Sarkar FH 2013. Overview of cancer stem cells (CSCs) and mechanisms of their regulation: Implications for cancer therapy. Curr Protoc Pharmacol. Chapter 14: Unit 14.25.

Begicevic RR and Falasca M 2017. ABC Transporters in cancer stem cells: Beyond chemoresistance. Int J Mol Sci. 18(11): 2362.

Berger K, Persson E, Gregersson P, Ruiz-mart S, Jonasson E, Ståhlberg A, Rhost S and Landberg G 2023. Interleukin-6 induces stem cell propagation through liaison with the sortilin – progranulin axis in breast cancer. Cancers 15(24): 5757.

Calcagno AM, Salcido CD, Gillet JP, Wu CP, Fostel JM, Mumau MD, Gottesman MM, Varticovski L and Ambudkar SV 2010. Prolonged drug selection of breast cancer cells and enrichment of cancer stem cell characteristics. J Natl Cancer Inst. 102(21): 1637–1652.

Cho Y and Kim YK 2020. Cancer stem cells as a potential target to overcome multidrug resistance. Front Oncol. 10: 541771.

Chong K, Chang Y, Hsu W, Tu Y, Chen Y, Lee M and Tsai K 2022. Breast cancer with increased drug resistance, invasion ability, and cancer stem cell properties through metabolism reprogramming. Int J Mol Sci. 23(21): 12875.

Clarke MF, Dick JE, Dirks PB, Eaves CJ, Jamieson CHM, Jones DL, Visvader J, Weissman IL and Wahl GM 2006. Cancer stem cells--perspectives on current status and future directions: AACR Workshop on cancer stem cells. Cancer Res. 66(19): 9339–9344.

Clements DN, Carter SD, Innes JF, Ollier WER and Day PJR 2006. Analysis of normal and osteoarthritic canine cartilage mRNA expression by quantitative polymerase chain reaction. Arthritis Res Ther. 8(6): R158.

Cocola C, Anastasi P, Astigiano S, Piscitelli E, Pelucchi P, Vilardo L, Bertoli G, Beccaglia M, Veronesi MC, Sanzone S, Barbieri O, Reinbold RA, Luvoni GC and Zucchi I 2009. Isolation of canine mammary cells with stem cell properties and tumour-initiating potential. Reprod Domest Anim. 44(Suppl 2): 214–217.

Fang M, Li Y, Huang K, Qi S, Zhang J, Zgodzinski W, Majewski M, Wallner G, Gozdz S, Macek P, Kowalik A, Pasiarski M, Grywalska E, Vatan L, Nagarsheth N, Li W, Zhao L, Kryczek I, Wang G and Wang L 2017. IL33 promotes colon cancer cell stemness via JNK activation and macrophage recruitment. Cancer Res. 77(10): 2735–2745.

Finetti F, Terzuoli E, Giachetti A, Santi R, Villari D, Hanaka H, Radmark O, Ziche M and Donnini S 2015. mPGES-1 in prostate cancer controls stemness and amplifies epidermal growth factor receptor-driven oncogenicity. Endocr Relat Cancer. 22(4): 665–678.

Fish EJ, Martinez-Romero EG, DeInnocentes P, Koehler JW, Prasad N, Smith AN and Bird RC 2020. Circulating microRNA as biomarkers of canine mammary carcinoma in dogs. J Vet Intern Med. 34(3): 1282–1290.

Fu J, Allen W, Xia A, Ma Z and Qi X 2014. Identification of biomarkers in breast cancer by gene expression profiling using human tissues. Genomics Data. 2: 299–301.

Griffiths-Jones S 2010. miRBase: microRNA sequences and annotation. Curr Protoc Bioinformatics. Chapter 12: Unit 12.9.1–10.

Hou Y, Li W, Sheng Y, Li L, Huang Y, Zhang Z, Zhu T, Peace D, Quigley JG, Wu W, Zhao Y and Qian Z 2015. The transcription factor Foxm1 is essential for the quiescence and maintenance of hematopoietic stem cells. Nat Immunol. 16(8): 810–818.

Hussen BM, Abdullah SR, Rasul MF, Jawhar ZH, Faraj GSH, Kiani A and Taheri M 2023. MiRNA-93: A novel signature in human disorders and drug resistance. Cell Commun Signal. 21(1): 1–24.

Im KS, Jang YG, Shin JI, Kim NH, Lim HY, Lee SM, Kim JH and Sur JH 2015. CD44+/CD24– cancer stem cells are associated with higher grade of canine mammary carcinomas. Vet Pathol. 52(6): 1041–1044.

Janakiram NB, Mohammed A, Bryant T, Ritchie R, Stratton N, Jackson L, Lightfoot S, Benbrook DM, Asch AS, Lang ML and Rao CV 2017. Loss of natural killer T cells promotes pancreatic cancer in LSL-Kras G12D/+ mice. Immunology. 152(1): 36–51.

Jansson MD and Lund AH 2012. MicroRNA and cancer. Mol Oncol. 6(6): 590–610.

Jiang S, Chen H, He K and Wang J 2022. Human bone marrow mesenchymal stem cells-derived exosomes attenuated prostate cancer progression via the miR-99b-5p/IGF1R axis. Bioengineered 13(2): 2004–2016.

Johnson-Arbor K and Dubey R 2023. Doxorubicin. In: XPharm: The Comprehensive Pharmacology Reference. SJ Enna and DB Bylund (eds.). 1–5.

Jovanović B, Beeler JS, Pickup MW, Chytil A, Gorska AE, Ashby WJ, Lehmann BD, Zijlstra A, Pietenpol JA and Moses HL 2014. Transforming growth factor beta receptor type III is a tumor promoter in mesenchymal-stem like triple negative breast cancer. Breast Cancer Res. 16(4): 1–14.

Kaltschmidt C, Banz-Jansen C, Benhidjeb T, Beshay M, Förster C, Greiner J, Hamelmann E, Jorch N, Mertzlufft F, Pfitzenmaier J, Simon M, Schulte Am Esch J, Vordemvenne T, Wähnert D, Weissinger F, Wilkens L and Kaltschmidt B 2019. A role for NF-κB in organ specific cancer and cancer stem cells. Cancers 11(5): 655.

Kang SJ, Gu NY, Byeon JS, Hyun BH, Lee J and Yang DK 2023. Immunomodulatory effects of canine mesenchymal stem cells in an experimental atopic dermatitis model. Front Vet Sci. 10: 1201382.

Kudaravalli S, den Hollander P and Mani SA 2022. Role of p38 MAP kinase in cancer stem cells and metastasis. Oncogene 41(23): 3177.

Liu WG, Zhuo L, Lu Y, Wang L, Ji YX and Guo Q 2020. miR-874-3p inhibits cell migration through targeting RGS4 in osteosarcoma. J Gene Med. 22(9).

Louie E, Nik S, Chen J-S, Schmidt M, Song B, Pacson C, Chen XF, Park S, Ju J and Chen EI 2010. Identification of a stem-like cell population by exposing metastatic breast cancer cell lines to repetitive cycles of hypoxia and reoxygenation. Breast Cancer Res. 12(6): R94.

Lu XY and Jin H 2024. MiRNAs function in the development of resistance against doxorubicin in cancer cells: targeting ABC transporters. Front Pharmacol. 15: 1–26.

Magalhães GM, Terra EM, de Oliveira Vasconcelos R, de Barros Bandarra M, Moreira PRR, Rosolem MC and Alessi AC 2013. Immunodetection of cells with a CD44+/CD24- phenotype in canine mammary neoplasms. BMC Vet Res. 9: 205.

Mengistu BA, Tsegaw T, Demessie Y, Getnet K, Bitew AB, Kinde MZ, Beirhun AM, Mebratu AS, Mekasha YT, Feleke MG and Fenta MD 2024. Comprehensive review of drug resistance in mammalian cancer stem cells: implications for cancer therapy. Cancer Cell Int. 24(1): 406.

Michishita M, Akiyoshi R, Suemizu H, Nakagawa T, Sasaki N, Takemitsu H, Arai T and Takahashi K 2012. Aldehyde dehydrogenase activity in cancer stem cells from canine mammary carcinoma cell lines. Vet J. 193(2): 508–513.

Moreira MP, da Conceição Braga L, Cassali GD and Silva LM 2018. STAT3 as a promising chemoresistance biomarker associated with the CD44+/high/CD24-/low/ALDH+ BCSCs-like subset of the triple-negative breast cancer (TNBC) cell line. Exp Cell Res. 363(2): 283–290.

Niture S, Gadi S, Qi Q, Gyamfi MA, Varghese RS, Rios-Colon L, Chimeh U, Vandana, Ressom HW and Kumar D 2023. MicroRNA-483-5p inhibits hepatocellular carcinoma cell proliferation, cell steatosis, and fibrosis by targeting PPARα and TIMP2. Cancers 15(6): 1715.

Oliveros JC 2015. Venny. An interactive tool for comparing lists with Venn's diagrams. [Online]. Available: http://bioinfogp.cnb.csic.es/tools/venny. Accessed November 6, 2019.

Ouzounova M, Vuong T, Ancey PB, Ferrand M, Durand G, Le-Calvez Kelm F, Croce C, Matar C, Herceg Z and Hernandez-Vargas H 2013. MicroRNA miR-30 family regulates non-attachment growth of breast cancer cells. BMC Genomics. 14: 139.

Pan X, Wang G and Wang B 2021. Ectopic expression of microRNA-874 represses epithelial mesenchymal transition through the NF-κB pathway via CCNE1 in cholangiocarcinoma. Cell Signal. 82: 109927.

Park EY, Chang E, Lee EJ, Lee H-W, Kang H-G, Chun K-H, Woo YM, Kong HK, Ko JY, Suzuki H, Song E and Park JH 2014. Targeting of miR34a-NOTCH1 axis reduced breast cancer stemness and chemoresistance. Cancer Res. 74(24): 7573–7582.

Peters IR, Helps CR, Calvert EL, Hall EJ and Day MJ 2005. Cytokine mRNA quantification in histologically normal canine duodenal mucosa by real-time RT-PCR. Vet Immunol Immunopathol. 103(1–2): 101–111.

Piva R, Spandidos DA and Gambari R 2013. From microRNA functions to microRNA therapeutics: novel targets and novel drugs in breast cancer research and treatment (Review). Int J Oncol. 43(4): 985–994.

Qin W, Ren Q, Liu T, Huang Y and Wang J 2013. MicroRNA-155 is a novel suppressor of ovarian cancer-initiating cells that targets CLDN1. FEBS Lett. 587(9): 1434–1439.

Rostoker R, Ben-Shmuel S, Rashed R, Shen Orr Z and LeRoith D 2016. CD24 cell surface expression in Mvt1 mammary cancer cells serves as a biomarker for sensitivity to anti-IGF1R therapy. Breast Cancer Res. 18(1): 51.

Rothschild SI 2014. microRNA therapies in cancer. Mol Cell Ther. 2(1): 7.

Rybicka A, Mucha J, Majchrzak K, Taciak B, Hellmen E, Motyl T and Krol M 2015. Analysis of microRNA expression in canine mammary cancer stem-like cells indicates epigenetic regulation of transforming growth factor-beta signaling. J Physiol Pharmacol. 66(1): 29–37.

Sahabi K, Selvarajah GT, Abdullah R, Cheah YK and Tan GC 2018. Comparative aspects of microRNA expression in canine and human cancers. J Vet Sci. 19(2): 162–171.

Sahabi K, Selvarajah GT, Ajat M, Abdullah R and Cheah YK 2022. Development and molecular characterization of doxorubicin-resistant canine mammary gland tumour cells. J Appl Anim Res. 50(1): 125–145.

Schultz NA, Dehlendorff C, Jensen BV, Bjerregaard JK, Nielsen KR, Bojesen SE, Calatayud D, Nielsen SE, Yilmaz M, Holländer NH, Andersen KK and Johansen JS 2014. MicroRNA biomarkers in whole blood for detection of pancreatic cancer. JAMA. 311(4): 392–404.

Selvarajah GT, Kirpensteijn J, van Wolferen ME, Rao NAS, Fieten H and Mol JA 2009. Gene expression profiling of canine osteosarcoma reveals genes associated with short and long survival times. Mol Cancer. 8: 72.

Song SJ, Poliseno L, Song MS, Ala U, Webster K, Ng C, Beringer G, Brikbak NJ, Yuan X, Cantley LC, Richardson AL and Pandolfi PP 2013. MicroRNA-antagonism regulates breast cancer stemness and metastasis via TET-family-dependent chromatin remodeling. Cell. 154(2): 311–324.

Tang B, Yoo N, Vu M, Mamura M, Nam JS, Ooshima A, Du Z, Desprez PY, Anver MR, Michalowska AM, Shih J, Parks WT and Wakefield LM 2007. Transforming growth factor-β can suppress tumorigenesis through effects on the putative cancer stem or early progenitor cell and committed progeny in a breast cancer xenograft model. Cancer Res. 67(18): 8643–8652.

Tang R, Yang C, Ma X, Wang Y, Luo D, Huang C, Xu Z, Liu P and Yang L 2016. MiR-let-7a inhibits cell proliferation, migration, and invasion by down-

regulating PKM2 in gastric cancer. Oncotarget 7(5): 5972–5984.

Tomiyasu H, Goto-Koshino Y, Takahashi M, Fujino Y, Ohno K and Tsujimoto H 2010. Quantitative analysis of mRNA for 10 different drug resistance factors in dogs with lymphoma. J Vet Med Sci. 72(9): 1165–1172.

Turna O, Uvez A, Baykal A, Sedef Develi E, Diramali M, Sonmez K, Karakas D, Kasikci G, Armutak EI and Ulukaya E 2023. Evidence for heterogeneity in response to treatment in mammary tumors of dogs as happens in humans. Vet Res Commun. 47(1): 111–120.

Xu E, Hu M, Ge R, Tong D, Fan Y, Ren X and Liu Y 2021. LncRNA-42060 Regulates Tamoxifen Sensitivity and Tumor Development via Regulating the miR-204-5p/SOX4 Axis in Canine Mammary Gland Tumor Cells. Front Vet Sci. 8: 1–15.

Yu L, Gulati P, Fernandez S, Pennell M, Kirschner L and Jarjoura D 2011. Fully Moderated T-statistic for Small Sample Size Gene Expression Arrays. Stat Appl Genet Mol Biol. 10(1): 42.

Yue Z, Yuan Z, Zeng L, Wang Y, Lai L, Li J, Sun P, Xue X, Qi J, Yang Z, Zheng Y, Fang Y, Li D, Siwko S, Li Y, Luo J and Liu M 2018. LGR4 modulates breast cancer initiation, metastasis, and cancer stem cells. FASEB J. 32(5): 2422.

Zadran S, Remacle F and Levine RD 2013. miRNA and mRNA cancer signatures determined by analysis of expression levels in large cohorts of patients. Proc Natl Acad Sci U S A. 110(47): 19160–19165.

Zambrano-Estrada X, Landaverde-Quiroz B, Dueñas-Bocanegra AA, De Paz-Campos MA, Hernández-Alberto G, Solorio-Perusquia B, Trejo-Mandujano M, Pérez-Guerrero L, Delgado-González E, Anguiano B and Aceves C 2018. Molecular iodine/doxorubicin neoadjuvant treatment impair invasive capacity and attenuate side effect in canine mammary cancer. BMC Vet Res. 14(1): 1–14.

Zhang B, Zhao R, He Y, Fu X, Fu L, Zhu Z, Fu L and Dong J-T 2015. Micro RNA 100 sensitizes luminal A breast cancer cells to paclitaxel treatment in part by targeting mTOR. Oncotarget 7(5): 5702–5714.

Zhao L, Qiu T, Jiang D, Xu H, Zou L, Yang Q, Chen C and Jiao B 2020. SGCE promotes breast cancer stem cells by stabilizing EGFR. Adv Sci (Weinh). 7(14): 1903700.

Zhou B, Jin Y, Zhang D and Lin D 2018. 5-Fluorouracil may enrich cancer stem cells in canine mammary tumor cells in-vitro. Oncol Lett. 15(5): 7987-7992.